Journal of the Indian Society of Remote Sensing (April 2020) 48(4):689–707
https://doi.org/10.1007/s12524-019-01097-0

COVER ARTICLE

# A Review of RUSLE Model

Kaushik Ghosal[1] · Santasmita Das Bhattacharya[1]

Received: 22 March 2019 / Accepted: 26 December 2019 / Published online: 11 January 2020


**Abstract**
In this paper, we attempted to review the soil erosion studies conducted throughout the globe using Revised Universal Soil Loss Equation (RUSLE). We searched the SCI, Scopus, Web of Science, Google Scholar database and various theses for this study. Though RUSLE is the most widely used model for estimation of soil erosion, the factors, namely rainfall erosivity, soil erodibility, slope length and steepness, cover management and conservation practice; vary greatly over different climatic zones, soil properties, slope, land cover and crop phase, respectively. Depending upon those variations, researchers have developed various sets of equation for different factors of RUSLE. These equations can be useful to map soil loss for many places on this planet.

**Keywords** RUSLE for soil erosion · Rainfall erosivity factor ($R$) · Soil erodibility factor ($K$) · Slope length and steepness factor (LS) · Cover management factor ($C$) · Conservation practice factor ($P$)

Revised Universal Soil Loss Equation (RUSLE) is a well-known and universally accepted and implemented empirical soil erosion estimation model. The RUSLE model is developed based upon five factors—(1) rainfall erosivity factor ($R$), (2) soil erodibility factor ($K$), (3) slope length and steepness factor (LS), (4) cover management factor ($C$) and (5) conservation practice factor ($P$) for the estimation of the average annual soil loss ($A$).

$$A = R\,K\,LSC\,P \tag{1}$$

The rainfall erosivity factor ($R$) evaluates the effect of rainfall impact in the form of kinetic energy, and it also predicts the rate and amount of run-off which is directly interconnected with that precipitation event. In their work, Wischmeier and Smith (1957) wrote, one hundredth of the product of kinetic energy of the storm and the 30-min intensity, which is expressed as $EI_{30}$, gives the most reliable result in the estimation of rainfall erosion potential. The total annual EI value is defined as the rainfall erosion index.

✉ Santasmita Das Bhattacharya
santasmita@gmail.com

Kaushik Ghosal
Kaushikghosal02@gmail.com

[1] Department of Mining Engineering, Indian Institute of Engineering Science and Technology, Shibpur, P.O. - Botanic Garden, Howrah, West Bengal 711103, India

The soil erodibility factor ($K$) shows the resistance of soil against erosion due to the impact of raindrop and the rate and amount of run-off produced for that rainfall impact, under a standard condition. As per Schwab et al. (1994), soil erodibility depends upon geological and soil features like structure, texture, inherent material, porosity, organic content, etc. Although the presence of sand and clay percentage is huge, soils become highly erodible if the presence of silt percentage is high (Mhangara et al. 2012).

The slope length ($L$) and steepness ($S$) factor reflect the effect of regional topography on the rate of soil erosion as the merged effects of length of the slope ($L$) and the steepness of the slope ($S$). As the length of the slope increases, the amount and rate of cumulative run-off increase. As the land slope increases, the run-off velocity also increases and that causes huge erosion.

The soil loss is highly dependent upon amount and type of vegetation cover (Benkobi et al. 1994). Basically, the vegetation cover prevents the raindrops to impact on soil surface and dissipates the kinetic energy of rainfall before reaching the surface of the soil. The cover management factor ($C$) is directly influenced with the vegetation type, stage of growth of the vegetation and percentage of vegetation cover.

The conservation or support practice factor ($P$) shows the effects of implementations that will reduce the rate and amount of the run-off, and thus, it reduces the amount and rate of soil erosion. The $P$ factor reflects the proportion of

soil loss for a particular support practice present for the corresponding soil loss with the presence of upward and downward slope, contour farming and tillage practice (Wischmeier and Smith 1957) (Renard et al. 1997). Strip cropping, contour farming, terracing, cross-slope cultivation and grassed waterways are the major support practices. As per Gitas (2009), the *P* values are calculated as the ratio of the rate and amount of soil loss due to a specific support practice to the soil loss due to row farming in upward and downward of the slope condition.

The major factors which affect soil erosion are the amount and intensity of rainfall on an area which directly implies the impact of raindrop on surface of the soil, causing erosion, and the *R* factor is the measure of that rainfall erosivity. Another major soil erosion influencing factor is *K* factor which shows the potential of soil to withstand against the impact of rain droplet. Other factors also have massive influence on soil erosion.

## Variation of Rainfall Erosivity Factor (*R*) Over Different Climatic Zones

### Application of RUSLE Over Tropical Wet Climatic Zones

The tropical climatic zones are found around the equatorial region. In these climatic zones, the warm temperature exists throughout the year. In the equator, the warm air rises. As it rises up, it cools down which causes rainfall. Tropical climates are generally two types—wet tropical climates and wet and dry tropical climates. Tropical wet climates occur at or very near the equator. Massive rainfall exists throughout the year.

As this climatic region is highly moist and rainfall impacts are quite high, Ranzi et al. (2012) used the *R* factor developed by Loureiro and Coutinho (2001):

$$R = \frac{1}{N}\sum_{i=1}^{N}\left(\sum_{m=1}^{12}(7.05\,\text{rain}_{10} - 88.92\,\text{days}_{10}\right)m,i) \quad (2)$$

where $N$ is the number of years of observations, $\text{rain}_{10}$ is monthly rainfall only when rainfall $\geq$ 10 mm, otherwise $\text{rain}_{10}$ is set to zero. $\text{Day}_{10}$ is the number of days in a month when rainfall $\geq$ 10 mm. This above equation produces a high level of erosion potential of rainfall with huge monthly rainfall (i.e. rain10). It also shows that, for a given rainfall amount, if the no. of rainy days is decreased (i.e. days 10), the rainfall intensity and erosion potential will increase, as expected. The monthly rainfall erosivity factor of the Lo river basin, Vietnam, was computed using this equation.

Adediji et al. (2010) used equation developed by Roose (1996) for Katsina, Nigeria, West Africa:

$$R_{10} = r \times a \quad (3)$$

where $R_{10}$ is the main annual rainfall erosivity factor over 10 years, r is the mean annual rainfall, $a$ = 0.05 in general, $a$ = 0.6 near the marine region (< 40 km), $a$ = 0.3 to 0.2 for tropical mountainous regions, $a$ = 0.1 in mountainous areas of Mediterranean region.

Agele et al. (2013) for his study over Pahang river basin, Malaysia, used the equation developed by Kassam (1992):

$$R = 117.6 \times (1.00105\text{^}(\text{AAP})) \quad (4)$$

where AAP is the annual average precipitation.

In India, Prasannakumar et al. (2011) used the equation which was developed by Arnoldus et al. (1980) for Siruvani river watershed, Attapady valley, Kerala.

$$R = \sum_{i=1}^{12} 1.735 \times 10^{\left(1.5\log_{10}\left(\frac{P_i}{P}\right)-0.08188\right)} \quad (5)$$

where $R$ is rainfall erosivity factor (MJ mm $\text{ha}^{-1}$ $\text{h}^{-1}$ $\text{year}^{-1}$); $P_i$ is monthly rainfall (mm); $P$ is an annual rainfall (mm).

Baby and Nair (2016) used it for Kuttiyadi river basin, Northern Kerala, India; Markose and Jayappa (2016a, b) applied this equation for Kali river basin, Karnataka, India; Ganasri and Ramesh (2016) used it for Nethravathi Basin, middle region of Western Ghats, India. This equation shows the weighted average concept of precipitation, so this equation can also be applied in other climatic conditions.

### Application of RUSLE Over Tropical Wet and Dry Climatic Zones

Tropical wet and dry climate is prevailing between 5° and 20° latitudes and receives less rainfall. Mainly in this type of climatic zone, rainfall occurs in a particular (i.e. single) season but the rest of the seasons becomes dry.

In this less moist climatic zone due to the lack of rainfall, there is a great variation in *R* factor calculation. For Ethiopian climatic condition, Hurni (1985) adopted a model that was based on the convenient annual average rainfall data of that area. The equation is expressed as:

$$R = -8.12 + (0.562 \times P) \quad (6)$$

where $R$ is rainfall erosivity factor and $P$ is the available average annual rainfall data. Gelagay (2016) used the model developed by Hurni (1985) for Koga watershed, Upper Blue Nile Basin, Ethiopia, North East Africa, and Gashaw et al. (2017a, b) used this model for Geleda watershed, Ethiopia.

Based on the study over the vast regions of Ivory Coast (Côte d'Ivoire) and Burkina Faso, Roose (1975) evaluated that mean annual EI30 values (i.e. the total kinetic energy due to impact of rainfall, where E is the total storm kinetic energy (MJ $ha^{-1}$), $I_{30}$ is the maximum of 30-min rainfall intensity in mm $h^{-1}$) can be approximated by multiplying the average annual rainfall totals (mm) with 50. Roose (1975) proposed this formula to estimate of *R* factor for RUSLE. In 1986, Morganhas used 0.5 as the general constant for multiplying the mean annual rainfall.

$$R = P \times 0.5 \tag{7}$$

*P* is the available mean annual rainfall data.

Morgan and Davidson (1991) again applied this model in Ivory Coast and Burkina Faso for their study. In India, Joshi et al. (2016) used this model for his study in the north of Pune, Maharashtra. In Kaas Plateau of Maharashtra, Dahe and Borate (2015) also applied this model.

Another model of *R* factor was developed by Singh (1981) as follows:

$$R = 79 + 0.363\,\mathrm{AAP} \tag{8}$$

where '*R*' is the rainfall erosivity factor, 'AAP' is the average annual precipitation in mm.

Vinay and Mahalingam (2015) used Singh's (1981) model for his study on Pandavapura, Mandya, Karnataka, India; Das and Guchait (2016) used it in Kharkai river basin, Jharkhand, India.

The equation developed by Arnoldus et al. (1980) as discussed previously, has been applied by Shit et al. (2015) for interfluve region of Kasai–Subarnarekha river, Jhargram, West Bengal, India. In 2016, Samanta et al. applied it for Subarnarekha river basin area, India.

## Application of RUSLE Over Semi-Arid or Steppe Climatic Zones

In semi-arid climatic zones, the amount of precipitation is below potential evapotranspiration. The variation in different kinds of semi-arid climate is depending upon variation of temperature which reflects the growth of different types of ecology.

Bu et al. 2003, developed *R* factor model for arid and semi-arid climatic zones mainly for China:

$$R_j = (0.1281 \times I_{30B} \times P_f) - (0.1575 \times I_{30B}) \tag{9}$$

where $P_f$ is annual rainfall (mm), *R* is mean annual rainfall erosivity factor (MJ mm $ha^{-1}$ $h^{-1}$ $year^{-1}$) and $I_{30B}$ is a storm's maximum 30-min intensity (mm/h.). The factor $I_{30B}$ indicates that as this zone is in lack of rainfall, Bu et al. (2003) and Foster et al. (1977) used maximum intensity of continuous 30-min rainfall; otherwise, all other individual rainfall intensities will be very much negligible. Chen et al. (2011) used this model in Miyun reservoir watershed, northern Beijing, North China.

In Xu et al. 2007, developed *R* factor model for this climatic zone using 2894 rainfall events over 25 years in 10 hydrologic gauge stations to build and compare monthly rainfall erosivity using daily rainfall data and monthly rainfall data of Beijing, respectively. The results from this two models show that they have similarity in precision with $R^2$ equal to 0.72. So the value of *R* factor was calculated according to Xu et al.'s (2007) equation:

$$R_m = 0.689P^{1.474} \tag{10}$$

Xu et al. (2013) used his above equation several times for Yangtze River Delta and Pearl River Delta of China.

In eastern Africa, Angima et al. (2003) used the model of Renard et al. (1997) in Kianjuki catchment, Embu, Central Kenya.

$$R = \frac{1}{n}\sum_{j=1}^{n}\left[\sum_{k=1}^{m}(E_k I_{30})\right]j \tag{11}$$

where *E* is the total kinetic energy produced by the rainfall (MJ $ha^{-1}$), $I_{30}$ is the maximum of 30-min rainfall intensity (mm $h^{-1}$), *j* is an index which shows the number of years used to generate the mean of rainfall data, k is an index which shows the number of storms occurred in a year, *n* is the number of years used to obtain the rainfall erosivity factor (*R*) and m is the number of storms occurs in a year. The total kinetic energy (*E*) generated by the rainfall impact is evaluated using the relation:

$$E = \sum_{j=1}^{m} e_r \Delta V_r \tag{12}$$

where $e_r$ is the rainfall energy generated per unit depth of rainfall per unit area in megajoules per hectare per millimetre (MJ $ha^{-1}$ $mm^{-1}$) and $\Delta V_r$ is the depth of rainfall in millimetres (mm) for the r-th increment of the storm hyetograph. This hyetograph is divided into m parts, in which each part will be having constant rainfall. Rainfall energy ($e_r$) generated per unit depth of rainfall, *er*, was evaluated using the relation:

$$e_r = 0.29\left[1 - 0.72\,e^{(-0.05\mathrm{ir})}\right] \tag{13}$$

where $e_r$ is units of megajoules per hectare per millimetre of rain (MJ $ha^{-1}$ $mm^{-1}$) and $i_r$ is rainfall intensity (mm $h^{-1}$). The intensity of rainfall for a particular increment of a rainfall event ($i_r$) is calculated using the relation:

$$i_r = \frac{\Delta Vr}{\Delta tr} \tag{14}$$

where $\Delta t_r$ is the duration of the increment of rainfall over which rainfall intensity is considered to be constant which

is in hour (h) and $\Delta Vr$ is the depth of rain falling (mm) during the increment.

Simms et al. (2003) adopted the model developed by Renard et al. (1997) for his study in the catchment of Lake Wollumboola, south of Sydney, and just north of Jervis Bayon, the New South Wales South Coast, Australia.

As discussed previously, Arnoldus et al. (1980) model of weighted average is also used in semi-arid or steppe climatic zones of India. Kartic et al. (2014) used this model in Kothagiri Taluk, Nilgiri, Tamil Nadu. Rahaman et al. (2015) applied this model in Kallar watershed, Western Ghats, north-west part of the Tamil Nadu.

## Application of RUSLE Over Humid Subtropical Climatic Zones

In humid subtropical climatic zone, the summer is highly humid and hot but the winter is very mild. These climate zones are usually located on the south-eastern side of all continents, usually between the latitudes of 25° and 35° and are located pole ward of neighbouring tropical climates. Other areas have more even or varying rain cycles, but regularly predictable dry summer months are missing. Most of the summer rains occur during thunderstorms, which build up due to the intensive surface heating and the strong subtropical sun angle. The weak tropical lows coming from adjacent warm tropical oceans, as well as rare tropical storms, often contribute to the seasonal rains of the summer. Winter rains take place with huge storms in the west winds, with fronts ranging in subtropical latitudes.

The Secretaria de Agricultura y Recursos Hidraulicos (1991) adopted processes developed by Wischmeier and Smith (1978a, b) to calculate the $EI_{30}$ values. After that, the annual precipitation was compared with these values to yield rainfall and run-off factor as follows:

$$R = -0.0334P_a + 0.006661P_a^2 \quad (15)$$

where $R$ represents the rainfall and run-off factor (MJ mm $ha^{-1}$ $h^{-1}$ $year^{-1}$) and $P_a$ is the measured annual precipitation in millimetres. Millward and Mersey (1999) applied Secretaria de Agricultura y Recursos Hidraulicos (1991) model in Zenzontla sub-catchment, Rio Ayuquila watershed, south-western Mexico, USA. In India, Naqvi et al. (2012) adopted this model for Nun river watershed, Dehradun, Uttarakhand.

The rainfall erosivity equation is generated for Australian tropical climate by Yu and Rosewell (1998) which is adopted by Xu et al. (2013) for Bohai Rim, China.

$$E_j = \alpha\,[1 + \eta\cos(2\pi fj + \omega)]\sum_{d=1}^{N} R_d^{\beta}(R_d > R_0) \quad (16)$$

where $Ej$ is the monthly rainfall erosivity (MJ mm $ha^{-1}$ $h^{-1}$ $year^{-1}$), $R_d$ is the daily rainfall, $R_0$ is the daily rainfall threshold causing erosion, in general, $R_0$ 12.7 mm, $N$ are the days of monthly rainfall $\geq$ 12.7 mm. $f$ is the frequency, $f$ = 1/12, and ω equals to 5π/6. α, β, η are the model parameters; the relationship between α and β is shown in the formula where the average annual rainfall is above 1050 mm.

$$\log\alpha = 2.11 - 1.57\beta \quad (17)$$

The relationship between the annual rainfall $P$ and $\eta$ is given in the formula. $\beta$ values range from 1.2 to 1.8, and $\beta$ is taken as 1.5 in this study.

$$\eta = 0.58 + 0.25P/1000 \quad (18)$$

Renard and Freimund (1994) developed a new model after several regression analyses:

$$R = 587.8 - 1.219P + 0.004105P^2 \quad (19)$$

where $P$ is the annual rainfall (mm) and R is the rainfall erosivity (MJ mm $ha^{-1}$ $year^{-1}$). Bhandari and Darnsawasdi (2015) adopted this model for Phewa watershed, Nepal. Biswas and Pani (2015) used it for Barakar river basin, Jharkhand, India.

Zhao et al. (2004) developed another model for china:

$$R = 8.3462\,\mathrm{rain}_9^{1.2570} \quad (20)$$

Where $rain_9$ is the monthly rainfall for days with rainfall depth $\geq$ 9.0 mm. Fu et al. (2005)used this model in Yanhe watershed, China.

In 1992, researchers of Korea Institute of Construction Technology (KICT) developed a model for derivation of $R$ factor. Kim et al. (2012) used this model at the Samgwang mine, Korea, as this model gives an equation which is best suitable for mining area also. The equation is as follows:

$$R = 38.5 + 0.35 \times P_r \quad (21)$$

where $P_r$ is the average annual rainfall (in mm $year^{-1}$).

As this equation yields values that are 10 times greater than the results of other methods, the computed values were reduced by a factor of 10 (Kim et al. 2012). Lee and Lee (2006) applied this model in Bosung basin, Korea. In India, Chatterjee et al. (2014) adopted this equation for Upper Subarnarekha river basin, Jharkhand. Ghosh et al. (2015) applied this equation for Bakreshwar river basin, West Bengal. Though Jaipanda watershed, Bankura, West Bengal, is near to tropical wet and dry climatic zones, Pal and Shit (2017) applied this equation in their study over here also.

Demirci and Karaburun (2012) applied Arnoldus et al. (1980) modified Fournier's index (MFI) on Buyukcekmece Lake watershed, western Istanbul, Turkey, Europe.

$$F_{\mathrm{F}} = \frac{\sum_{j=1}^{N} F_{a,j}}{N} = \frac{1}{N}\sum_{j=1}^{N}\sum_{i=1}^{12}\frac{P_{ij}^2}{P} \quad (22)$$

$F_{\mathrm{F}}$ is the modified Fournier index (MFI). $P_{ij}$ is the rainfall depth in month/(mm) of the year $j$, and $P$ is the total rainfall of that same year.

$$R = (4.17F_F) - 152 \quad (23)$$

Babu et al. (2004) developed an equation for the estimation of $R$ factor for Damodar Valley, Jharkhand, India.

$$R = 81.5 + 0.375 \times r \quad (24)$$

where $340 \leq r \leq 3500$ mm.

In Tirkey et al. 2013, used Babu et al. (2004) equation for Daltonganj watershed, Palamu district, Jharkhand, India. Kamuju (2015) adopted this model for Gumani watershed, Jharkhand, India. As per their observation, Babu et al. (2004) model was highly suitable for Damodar Valley of eastern India and its neighbouring region.

But later on, Kamuju observed that the generalised models developed earlier by Babu et al. (1979) were more appropriate, as follows:

$$\mathrm{EI30} = 3.1 + 0.533 \times R_d(\text{for daily rainfall in mm}) \quad (25)$$

$$\mathrm{EI30} = 1.9 + 0.640 \times R_m(\text{for monthly rainfall in mm}) \quad (26)$$

For this reason, Kamuju applied this equation for his study area. Based on the above equations, Kamuju (2016) adopted the regression equation for $R$ factor determination in Asan watershed, Uttarakhand, India, as follows:

$$R = 22.8 + 0.6400 \times R_a \quad (27)$$

where $R$ is the rainfall erosivity factor (MJ mm ha$^{-1}$ - year$^{-1}$) and $R_a$ is the annual average rainfall (mm). Swarnkar et al. (2017) also used this equation in Garra/Deoha river basin, Uttarakhand, India.

The method developed by Singh (1981) (as discussed previously) was also used in this climatic zone by Parveen and Kumar (2012) for Upper South Koel Basin, Jharkhand, India. Agarwal et al. (2016) used it for Khajuri watershed, Barkachha, Mirzapur, Uttar Pradesh, India. From Singh's (1981) model concept, Kumar and Kushwaha (2013) generate a new set of equations as follows:

$$Y_1 = 79 + 0.383X_1 (r = 0.83) \quad (28)$$

$$Y_2 = 50 + 0.389X_2 (r = 0.88) \quad (29)$$

In the first equation, $Y_1$ is the annual average erosion index (m ha cm$^{-1}$) and $X_1$ is the average annual rainfall (mm), and in the second, $Y_2$ is the average seasonal erosion index and $X_2$ is the average seasonal rainfall (mm).

## Application of RUSLE Over Montane or Alpine Climatic Zones

In this climatic zone, the atmosphere is highly cold and arid. Basically, this climate is called as the average weather for the regions above the tree line. The amount of rainfall is very less.

Bhat et al. (2017) used Singh's (1981) (previously discussed) model in Kashmir, north-west India. Kalambukattu and Kumar (2017) used Babu et al.'s (2004) (previously discussed) model in Maniyar watershed, Uttarakhand, India.

## Application of RUSLE Over Mediterranean Climatic Zones

The Mediterranean climate is basically dry summer subtropical climate due to the presence of Mediterranean Sea beside this climatic zone. The wet winter with dry summer defines the characteristic of this climate. In this climatic zone, there exists seasonal precipitation regime.

R was computed using an empirical equation developed by ICONA (1988), which shows adequate results for the areas with an average annual rainfall of less than 500 mm:

$$R = 10fPI_{1.2}I_{24.2} \quad (30)$$

where $f$ is a zonal coefficient with the value of 0.00035, $P$ is the mean annual rainfall (mm), and $I_{1.2}$ and $I_{24.2}$ are the maximum rainfall intensity in 1-h duration and 24-h duration for the 2-year return period, respectively. Bonilla et al. (2010) used this empirical approximation in Santo Domingo County, Central Chile, South America.

Van et al. (2000) generated a new $R$ factor model for Italian Mediterranean climatic zones. The equation has been used in several studies (e.g. Zarris et al. 2011); (Sigalos et al. 2010)), performing exceptionally well under Mediterranean or more specifically Greek climatic conditions. The equation is as follows:

$$R = a.P \quad (31)$$

The "$a$" factor is equal to 1.3, and P is the average annual rainfall (mm).

Efthimiou et al. (2014) used this model for Venetikos river catchment, Macedonia, Greece, Europe.

Sorrentino (2001) also generated a new $R$ factor model for Italian Mediterranean climatic condition. In his model, he shows that kinetic energy is directly dependent on the altitude of that location.

$$R = (1163.45 + 4.9H - 35.2NGP - 0.58q)/100 \quad (32)$$

where $H$ (mm y$^{-1}$) is the annual average precipitation, NGP is the average of the rainy days per year and $q$ is the elevation of that site (from MSL). Terranova et al. (2009)

applied Sorrentino's (2001) model in Calabria, southern Italy, Europe.

With Italian Mediterranean rainfall regime, Diodato (2004) developed another model:

$$R = \frac{1}{N}\sum_{1}^{N} \mathrm{EI}_{30-\mathrm{annual}} \tag{33}$$

where $N$ is the number of the considered years.

Onori et al. (2006) used this model in Comunelli catchment, south-central Sicily, Italy. He used $\mathrm{EI}_{30-\mathrm{annual}} = 12.142(abc)^{0.6446}$ (MJ mm ha$^{-1}$ h$^{-1}$) as the annual erosive empirical index. $a$, $b$ and $c$ are expressed in centimetres, where '$a$' is the annual precipitation, '$b$' is the annual maximum daily precipitation and '$c$' is the annual maximum hourly precipitation. Variable '$a$' shows less erosive precipitations, with a cumulative effect over a long period. Variables '$b$' and '$c$' describe very erosive effects due to extreme rainfalls in storms and heavy showers.

Flabouris (2008) developed a model for Greece. Rozos et al. (2013) applied this model for North Euboea, Island, Greece, Europe.

$$R = R_n \times a \tag{34}$$

where '$a$' is equal to 0.5 for the study area. $R_n$ is the mean annual rainfall.

Previously used Arnoldus et al.'s (1980) modified Fournier's index (MFI) method was adopted by Ferro et al. (1991) for Sicily, Italy. Ferro et al. (1991) generated soil isoerosivity map which was used by Maria et al. (2009) in China, north-western Crete, Greece, Europe. Irvem et al. (2007) in his study on Seyhan river basin in Turkey observed that a relationship between R and F can be determined by regression analysis, and this relationship changes with the change in various climatic zones.

The basic equation generated by Renard et al. (1997) was also used by HAMMAD et al. (2005) in Ramallah, Palestine, Israel.

## Application of RUSLE Over Desert or Arid Climatic Zones

The desert climate is also known as an arid climate. In this climate, precipitation is too low to sustain any kind of vegetation.

Soil erosion due to the impact of rainfall is not so popular for desert climate as precipitation is mostly absent in this type of climate. Santra et al. (2014) applied a model in Jodhpur, western Rajasthan, India, which was developed by Irvem et al. (2007). This model was generated from the regression analysis of Arnoldus et al. (1980) modified Fournier's index (MFI) concept.

## Variation of Soil Erodibility Factor (*K*) Over Different Soil Properties in Consideration

The soil erodibility factor ($K$) is a significant influencing factor of RUSLE soil erosion estimation model. Soil erodibility relies on soil and/or geological characteristics, such as parent material, texture, structure (USDA 1951), organic matter content, porosity and catena (Schwab et al. 1994). Generally, soils show less erodibility if the silt concentration is low, regardless of the presence of high concentration in the sand and clay fractions. The developers choose and compare different properties and generate different soil $K$ factor models as per their suitability and requirement.

### *K* Factor on the Basis of Particle Size Distribution of Soil

El-Swaify and Dangler (1976) developed a model with respect to grain size distribution of soil (i.e. % sand, % silt, % clay in the soil) and the degree of saturation of the soil.

$$K = -0.03970 + 0.00311\mathrm{A}_1 + 0.00043\mathrm{A}_2 + 0.00185\mathrm{A}_3 + 0.00258\mathrm{A}_4 - 0.00823\mathrm{A}_5 \tag{35}$$

where $\mathrm{A}_1$ is the per cent unstable aggregates $< 0.250$ mm, $\mathrm{A}_2$ is the product of the per cent of silt (0.002–0.01 mm) and sand (0.1–2 mm) present in the sample, $\mathrm{A}_3$ is the per cent base saturation of the soil, $\mathrm{A}_4$ is the per cent silt present (0.002–0.050 mm) and $\mathrm{A}_5$ is the per cent sand in the soil (0.1–2 mm).

This equation results in a $K$ factor with units of ton acre hour per (hundred of acre feet tonf inch). To obtain the $K$ factor value in SI unit (Mg h MJ$^{-1}$mm$^{-1}$), this $K$ factor is divided by 7.59. Angima et al. (2003) used this model for the estimation of $K$ factor in Kenyan Highlands, Africa.

### *K* Factor on the Basis of Grain Size Distribution, Organic Content, Structural Class, Permeability Rate of Soil

Wischmeier and Smith (1978a, b) observed that soil erodibility factor is not only depending upon the particle size but it also depends on the amount of organic matter or carbon content in it, the molecular bonding or the structural class its belongs with and the rate of permeability it have. He developed a model equation and a nomograph on the basis of that equation.

$$K = \left[2.1 \times 10^{-4} M^{1.14}(12 - OM) + 3.25\,(S-2) + 2.5(p-3)\right]/759 \tag{36}$$

where OM = the organic content (%) of soil and M = grain size parameter that is the product of the silt content (%) (particles of 0.002 to 0.1 mm in diameter) with (100% clay). The '*s*' and '*p*' parameters describe soil structure and permeability, respectively. Parysow et al. (2003) used this model in Fort Hood, Texas, USA. Shi et al. (2004) used this model for Wangjiaqiao watershed, Zigui, Hubei, China. Chen et al. (2011) used in Miyun watershed, China. Lopez-Vicente et al. (2008) adopted this equation for Central Spanish Pyrenees. Bonilla et al. (2010) used this empirical model in Santo Domingo County, Central Chile, South America. In South Africa, Mhangara et al. (2012) adopted Wischmeier and Smith (1978a, b) modelling approach for Keiskamma catchment. In India, Naqvi et al. (2012) used this model in Nun river watershed, Dehradun, Uttarakhand. Kartic et al. (2014) used it for Kothagiri Taluk, Nilgiri, north-west part of the Tamil Nadu. Vinay and Mahalingam (2015) adopted it for his study on Pandavapura, Mandya, Karnataka. Joshi et al. (2016) used the model for his study in the north of Pune, Maharashtra. Markose and Jayappa (2016a, b) used it in Kali river basin, Uttara Kannada, Karnataka. Pal and Shit (2017) used it for Jaipanda watershed, Bankura, West Bengal. Swarnkar et al. (2017) used this model in Garra/Deoha river basin, Uttarakhand. Bhat et al. (2017) used it for Kashmir. In Nepal, Bhandari and Darnsawasdi (2015) adopted this model for Phewa watershed. Efthimiou et al. (2014) used this model for Venetikos river catchment, Western Macedonia, Northern Greece, Europe.

After Wischmeier and Smith (1978a, b) model, Schwab et al. (1981) developed another approach which was based on organic content and soil textural class. This model was adopted by Parveen and Kumar (2012) for Upper South Koel Basin, Jharkhand, India. Agarwal et al. (2016) applied this for his study in Khajuri watershed, Barkachha, Mirzapur, Uttar Pradesh, India.

Foster et al. (1981) developed another model from concepts of Wischmeier and Smith (1978a, b) nomograph:

$$K = \left[2.8 \times 10^{-7} M^{1.14}(12-a) + 4.3 \times 10^{-3}(b-2) + 3.3(c-3)\right] \quad (37)$$

where $K$ represents soil erodibility factor ($t$ ha$^{-1}$ per unit of $R$), $M$ represents particle size parameter (% silt + %very fine sand) × (100 − % clay), 'a' represents the content of organic matter (in%), '*b*' represents the structure code of soil and soil permeability class is represented by '*c*'. Kumar and Kushwaha (2013) used it in Pathri Rao subwatershed, Uttarakhand. Chatterjee et al. (2014) adopted this equation for Upper Subarnarekha river basin, Jharkhand. Kalambukattu and Kumar (2017) used this model in Maniyar watershed, Uttarakhand, India.

Goldman and Wischmeier (1986) developed a model which was almost similar to Wischmeier and Smith (1978a, b) equation:

$$K = 1.292\left[2.1 \times 10^{-6} f_p - 1.14 \times (12 - P_{\text{om}}) + 0.0325(S_{\text{str}} - 2) + 0.025(f_{\text{per}} - 3)\right] \quad (38)$$

where $K$ is soil erodibility factor in ton.h/MJ mm, $f_{\text{p}}$ is the particle size parameter, [$fp = (P_{\text{silt}} \times 100 - P_{\text{clay}})$], $P_{\text{om}}$ is per cent of organic matter, $S_{\text{str}}$ shows soil structural code (the $S_{\text{str}}$ values are as follows—for very fine granular $S_{\text{str}}$ is 1, for fine granular $S_{\text{str}}$ is 2, for moderate or coarse granular $S_{\text{str}}$ is 3, for blocky, platy or massive $S_{\text{str}}$ is 4), $f_{\text{per}}$ is profile permeability code (the $f_{\text{per}}$ values are as follows—for rapid $f_{\text{per}}$ is 1, for moderate to rapid $f_{\text{per}}$ is 2, for moderate $f_{\text{per}}$ is 3, for slow to moderate $f_{\text{per}}$ is 4, for slow $f_{\text{per}}$ is 5, for very slow $f_{\text{per}}$ is 6), $P_{\text{silt}}$ is per cent of silt, $P_{\text{clay}}$ is per cent of clay.

Dahe and Borate (2015) used this model in Kaas Plateau of Maharashtra, India.

Another model was developed by Sharpley and Williams (1990) considering top soil layer carbon content:

$$K = \{0.2 + 0.3\exp[0.0256\text{SAN}(1 - \text{SIL}/100)]\} \times \left(\frac{\text{SIL}}{\text{CLA} + \text{SIL}}\right)^{0.3} \times \left[1.0 - \frac{0.25C}{C + \exp(3.72 - 2.95C)}\right] \times \left[1.0 - \frac{0.7\text{SN}_1}{\text{SN}_1 + \exp(-5.51 + 2.95\text{SN}_1)}\right] \quad (39)$$

where SAN is the subsoil sand fraction, SIL is the subsoil silt fraction and CLA is the subsoil clay fraction (in %). C is the topsoil carbon content (in %). $\text{SN}_1 = 1 - \text{SAN}/100$.

Xu et al. (2013) adopted this model for Pearl River Delta and the Yangtze River Delta, China.Rosewell (1993) modified Wischmeier and Smith (1978a, b) model as follows:

$$K = \left\{2.77\left(10^{-7}\right)(12-\alpha)M^{1.14}\right\} + \left\{4.28\left(10^{-3}\right)(\beta-2)\right\} + \left\{3.29\left(10^{-3}\right)(\gamma-3)\right\} \quad (40)$$

where $M$ = {(% silt + % very fine sand). (100–% clay)}, α is organic matter (in%), $\beta$ is structure code and $\gamma$ is permeability rating.

Ganasri and Ramesh (2016) used it for Nethravathi Basin, middle region of Western Ghats, India.

Tew (1999) has done extensive work for the estimation of the soil erodibility factor to produce soil erodibility nomograph which was based on nomograph of Wischmeier and Smith (1978a, b) and he developed a model:

$$K = \left[\left(1.0 \times 10^{-4}\right)(12 - \mathrm{OM})M^{1.14} + 4.5(S-3) + 8(P-2)\right]/100 \quad (41)$$

where $K$ is soil erodibility factor (100ft.ton.in/acr.h) for SI unit (ton/ha)/(MJ mm ha$^{-1}$ h$^{-1}$). $M$ = (% silt + % very fine sand) × (100–% clay). OM is % of organic matter. $S$ is soil structure code. $P$ is permeability class. Agele et al. 2013 adopted (Tew 1999) model for his study in Pahang river basin, Malaysia.

Mulengera and Payton (1999) derived a model particularly based on Tanzanian tropical conditions:

$$K = 1.82247 \times 10^{-5} M + 0.0045 P_e - 0.0097 \quad (42)$$

where $K$ is soil erodibility factor in (ton ha hr ha$^{-1}$ - MJ$^{-1}$ mm$^{-1}$), $M$ = (si + vfs) × (si + vfs + sa); si: silt % (0.05–0.002 mm); sa: sand % (0.2–0.10 mm); vfs: very fine sand % (0.10–0.05 mm)

$P_e$ represents the permeability classes as follows: If, $P_e$ = 1 rapid (> 127 mm h$^{-1}$), 2 moderate to rapid (63.5–127 mm h$^{-1}$), 3 moderate (20–63.5 mm h$^{-1}$), 4 slow to moderate (5–20 mm h$^{-1}$), 5 slow (1–5 mm h$^{-1}$), 6 very slow (< 1 mm h$^{-1}$)

Vezina et al. (2006) used this model in Lo river basin, Viet Tri, north-east region of Vietnam, South East Asia.

### *K* Factor on the Basis of Soil Colour and Soil Type

Hurni (1985) and Helden (1987) suggested the soil erodibility values after observing soil colour (like black, red, brown) and soil type (Chromic Vertisols, Pellic Vertisols, Lithosols, Orthic Luvisols, Eutric Nitosols, Eutric Leptosols, Haplic Luvisols, Luvic Calcisols) that shows the soil erodibility of Highlands of Ethiopia. Amsalu and Mengaw (2014) applied this concept in Northwest Highlands of Ethiopia. Lema et al. (2016) adopted it for Ruba-Gered watershed, Ethiopia. Sewnet (2016) applied this method in Koga watershed, Upper Blue Nile Basin, Ethiopia. Gashaw et al. (2017a, b) also observed that the factors used by Wischmeier and Smith (1957) are difficult to estimate, so he used Hurni (1985) and Helden (1987) soil colour and chemical-type classification method in Geleda watershed, Blue Nile river basin, Ethiopia.

### *K* Factor on the Basis of Geometric Mean Particle Diameter

After considering all of the above methodologies developed by El-Swaify and Dangler (1976), Wischmeier and Smith (1978a, b), Hurni (1985) and Helden (1987); finally Renard et al. (1997) developed an empirical equation based on the geometric mean of particle diameter of soil. This method is highly used because the correlation ($R^2$) of its result with the field data is 0.983.

$$K = 0.0034 + 0.0405 \exp\left[-0.5\left(\frac{\log D_g + 1.659}{0.7101}\right)^2\right] \quad (43)$$

$$D_g = \exp\left[\sum 0.01 f_i \ln\{(d_{\max} + d_{\min})/2\}\right] \quad (44)$$

where $D$g represents geometric mean particle size (for clay, silt, sand), $d_{max}$ represents maximum diameter (mm), $d_{min}$ represents minimum diameter and $f_i$ represents corresponding fraction of mass.

Römkens et al. (1986) observed that this method gives the yield among others after performing world wide datasets. Van et al. (2000) adopted this equation for Italian soil erosion studies. Fu et al. (2005) used this model in Yanhe watershed, China. Onori et al. (2006) used this model in Comunelli catchment, south-central Sicily, Italy. Yue-Qing et al. (2008) used it for Maotiao river watershed, Guizhou, south-western China. Maria et al. (2009) applied it in Chania, north-western Crete, Greece, Europe.

Torri et al. (1997) introduced Naperian logarithm of the geometric mean of the particle size distribution. After several regression analyses, Torri et al. (1997) generated a model:

$$K = 0.0293(0.65 - D_G + 0.24 D_G^2 \times \exp\left\{-0.0021\left(\frac{\mathrm{OM}}{C}\right) - 0.00037\left(\frac{\mathrm{OM}}{C}\right)^2 - 4.02C + 1.72C^2\right\} \quad (45)$$

$$D_G = \sum_i f_i \log(d_{\max} \cdot d_{\min})^{0.5} \quad (46)$$

where $D_G$ is the Naperian logarithm of the geometric mean of the particle size distribution, $d_{max}$ is the maximum diameter (mm), $d_{min}$ is the minimum diameter, $f_i$ is the corresponding mass fraction. $C$ is the fraction of clay and OM is the percentage of organic matters.

Demirci and Karaburun (2012) applied it on Buyukcekmece Lake watershed, western Istanbul, Turkey, Europe. Santra et al. (2014) applied this model in Jodhpur, western Rajasthan, India.

After analysing many applications of RUSLE globally, it is observed that the major variation in methodologies is on the application of rainfall erosivity factor and soil erodibility factor which varies mainly on climatic condition and soil characteristic regression on soil properties, respectively. The other factors like slope length and steepness factor, conservation practice factor and cover management factor all are highly important, but there is not so much variation in development of these factors. The variation in these factors is discussed as below:

## Variation of Slope Length and Steepness Factor (LS)

The LS factor shows the combining effect of slope length ($L$) and slope steepness ($S$) that shows the topographical influences on soil erosion. As the length of the slope increases, the amount and rate of cumulative run-off increase. Also with an increase in slope of the land, the velocity of the run-off increases which contributes to erosion. The major variation in slope length and steepness factor lies within the variation of the slope steepness factor ($S$). We will see that the slope length factor ($L$) in each and individual model is same which is developed by Wischmeier and Smith (1957) and expressed as:

$$L = \left(\frac{\lambda}{\Psi}\right)^{m} \tag{47}$$

where $\lambda$ denotes the flow path length ($m$ or feet), the value of $\Psi$ is 22.13 for SI units and 72.6 for English units (BU) as the LS factor is the ratio per unit area of soil loss from a field slope to that from a 22.13 m length. The factor m varies in different model conditions. But the slope steepness factor ($S$) is highly variable. The variation in different models is discussed as follows:

## Wischmeier and Smith Slope Length and Steepness Factor (LS)

Wischmeier and Smith (1957) first developed LS factor, a dimensionless factor where $L$ is defined as the relative slope length (metres), taking the basic slope length as 22 m and basic slope gradient as 9% which leaves the LS values essentially unchanged. The LS factor is expressed as:

$$\mathrm{LS} = \left(\frac{\lambda}{\Psi}\right)^{m} . \left(0.065 + 0.046s + 0.0065s^{2}\right) \tag{48}$$

where $\lambda$ is the flow path length ($m$ or feet) which is denoted as $\lambda$ = (flow accumulation × cell size), the value of $\Psi$ is 22.13 for SI units and 72.6 for English units (BU) as the (LS) factor is the ratio of soil loss per unit area from a field slope to that from a 22.13 m length. $S$ is average slope gradient (%)

$m$ = 0.2 for $s < 1$, 0.3 for $1 \leq s < 3$, 0.4 for $3 \leq s < 5$, 0.5 for $5 \leq s < 12$ and 0.6 for $s \geq 12\%$

Wischmeier and Smith (1957) modified this above model replacing average slope gradient percentage (%) with sine of the slope angle ($\theta$).

$$\mathrm{LS} = \left(\frac{\lambda}{\Psi}\right)^{m} . \left(65.41 \sin^{2}\theta + 4.56 \sin\theta + 0.065\right) \tag{49}$$

where $\theta$ is the slope angle. The value of 'm' is 0.5 if the slope is 5% or more, 'm' is 0.4 if the slope is 3.5–4.5%, 'm' is 0.3 if the slope is 1–3%, and '$m$' is 0.2 on uniform where slope is less than 1%. The values for concave, convex or mixed-gradient slopes have been discussed in the form of a graph discussed by Wischmeier and Smith (1978a, b).

Rozos et al. 2013 applied this model for North Euboea, Island, Greece, Europe. Agele et al. 2013 used this model for his study over Pahang river basin, Malaysia. In India, Chatterjee et al. (2014) adopted this equation for Upper Subarnarekha river basin, Jharkhand. Ghosh et al. (2015) applied this equation for Bakreshwar river basin, West Bengal. Rahaman et al. (2015) applied this model in Kallar watershed, eastern part of Western Ghats, north-west part of the Tamil Nadu. Ganasri and Ramesh (2016) used it for Nethravathi Basin, middle region of Western Ghats, India. Agarwal et al. (2016) used it for Khajuri watershed, Barkachha, Mirzapur, Uttar Pradesh, India. Gashaw et al. (2017a, b) used this model for Geleda watershed, Blue Nile basin, Ethiopia.

For slopes up to 21%, the equation modified by Wischmeier and Smith (1957) can be applied, but for slope steepness of 21% or more the following equation has been used (Gaudasasmita 1987):

$$\mathrm{LS} = \left(\frac{\lambda}{\Psi}\right)^{0.7} . \left(6.432 \times \sin\left(\theta^{0.79}\right) \times \cos\theta\right) \tag{50}$$

Irvem et al. (2007) in his study on Seyhan river basin in Turkey used this concept. Santra et al. (2014) applied this model in Jodhpur, western Rajasthan, India. (Shinde et al. (2010) used it for Damodar Valley Catchment, Jharkhand, India.

## Moore and Burch Slope Length and Steepness Factor (LS)

On the basis of unit stream theory, Moore and Burch (1986) developed another model. This model's conceptualisation was that a unit mass of water in a natural stream is the only source of energy. This can have its potential energy above a datum. This unit mass of water releases its potential energy to transport sediment and creates its own channel as it flows down the gradient. It is reasonable to suspect that the rate of energy expenditure is related to the sediment transport.

$$\mathrm{LS} = \left(\frac{\lambda}{\Psi}\right)^{m} \left(\frac{\sin\beta}{0.0896}\right)^{n} Z \tag{51}$$

where $\lambda$ is flow path length (m or feet), $\lambda$ = (flow accumulation × cell size), the value of $\Psi$ is 22.13 for SI units and 72.6 for English units (BU) as the (LS) factor is the ratio of soil loss per unit area from a field slope to that from a 22.13 m length. $\beta$ is slope angle in radian (i.e. $\beta = 3.14 \times \theta/180$ where θ is the slope angle in degree.).

$Z = (c/e)^{0.4}$; it is defined as rilling factor. Rilling factor is used to modify the length slope factor which is developed from the theory of unit stream power. If sheet flow occurs, $J = 1$, $c = 1$, and $e = 1$ so that $Z = 1$. In the absence of any parabolic-shaped rill per unit length of the contour element, with a top width of 20 cm, then $J = 1$, $c = 2/3$, and $e = 0.2$, so that $Z = 1.62$. Finally, if there exist five parabolic rills per unit length of the contour element, each with a top width of 10 cm, then $J = 5$, $c = 2/3$, and $e = 0.5$, so that $Z = 1.12$; where $J$ denotes the number of rills crossing the contour element and c and e are constants.

Moore and Burch (1986) assumed that the value of 'c' is 1 for a rectangular cross section, the value of 'c' is 2/3 for a parabolic cross section, and $c = 1/2$ for a triangular cross section. The coefficient m and n varies in different studies. Mainly Moore and Burch (1986) explained $m = 0.4$ and $n = 1.3$, but many researchers have changed it as per their suitable conditions. It is observed that the rilling factor ($Z$) is taken either 1 or 1.4 in each study. This particular model is used by Van et al. (2000) for his study in Italy. In southern India, Prasannakumar et al. (2011), Vinay and Mahalingam (2015), Baby and Nair (2016) and Markose and Jayappa (2016a, b) used this equation for Siruvani river watershed, Attapady valley, Kerala; Pandavapura, Mandya, Karnataka; Kuttiyadi river basin, Northern Kerala; and Kali river basin, Karnataka, respectively. Das and Guchait (2016) used it in Kharkai river basin, Jharkhand, India. Bhat et al. (2017) used for Kashmir Valley, India. All of the above researchers have taken $m = 0.4$ and $n = 1.3$ as per Moore and Burch (1986).

Simms et al. (2003) adopted this model for his study in the catchment of Lake Wollumboola, New South Wales, Australia. There were various usages of this model in different states of India. In Jharkhand, Parveen and Kumar (2012) and Tirkey et al. (2013) used this equation for Upper South Koel Basin and Daltonganj watershed, Palamu district, respectively; in Maharashtra, Dahe and Borate (2015) and Joshi et al. (2016) used this equation for Kaas Plateau and Pune, respectively; in Uttarakhand, Kumar and Kushwaha (2013) and Kalambukattu and Kumar (2017) used model it for Pathri Rao sub-watershed and Maniyar watershed, respectively. All of the above researchers have taken $m = 0.6$ and $n = 1.3$ (Moore and Burch 1986).

In Jharkhand, India, Samanta et al. (2016) and Kamuju (2015) applied this model for Subarnarekha river basin and Gumani watershed, respectively; Pal and Shit (2017) used it for Jaipanda watershed, Bankura, West Bengal; Ramu and Mahalingam (2015) used it for Pandavapura, Mandya, Karnataka. In their study, they used $m = 0.4$ and $n = 1.4$.

Adediji et al. (2010) used Katsina, Nigeria, West Africa, with $m = 0.4$ and $n = 1.1$.

Terranova et al. (2009) applied this model in Calabria, southern Italy, Europe. Here he used $m = (0.1–0.6)$ and $n = (1–1.4)$ with very sensitive field study.

## McCool, Foster, Weesies Slope Length and Steepness Factor (LS)

By using step coupling methods, McCool et al. (1987) developed another slope steepness factor model and also used the slope length model developed by Wischmeier and Smith (1957).

$$\mathrm{LS} = L \times S \tag{52}$$

where $L = \left(\frac{\lambda}{\Psi}\right)^m$, $\lambda$ is flow path length (m or feet), $\lambda$ = (flow accumulation × cell size), $\Psi = 22.13$ for SI units and 72.6 for English units (BU) as the (LS) factor is the ratio of soil loss per unit area from a field slope to that from a 22.13 m length.

$$m = \frac{(\sin\theta/0.0896)/[3 \times (\sin\theta)0.8 + 0.56]}{1 + (\sin\theta/0.0896)/[3 \times (\sin\theta)0.8 + 0.56]} \tag{53}$$

$$S = \begin{cases} 10.8\ \sin\theta + 0.03\ \theta < 5^\circ \\ 16.8\ \sin\theta - 0.55^o \leq \theta < 10^\circ \\ 21.9\ \sin\theta - 0.96\ \theta \geq 10^\circ \end{cases} \tag{54}$$

where $\theta$ is the slope angle in degree. Angima et al. (2003) used this model in Kenyan Highlands, Africa. Hammad et al. (2005) used this model in Ramallah, Palestine, Israel. Xu et al. (2013) adopted this model for Bohai Rim, China. In India, Shit et al. (2015) used it for Kasai-Subarnarekha river interfluves zone Jhargram subdivision, West Bengal; Samanta et al. (2016) applied it for Subarnarekha river basin, Jharkhand; Swarnkar et al. (2017) used this model in Garra/Deoha river basin, Uttarakhand.

Hickey (2000) and Van et al. (2001) developed the advanced software modelling version of McCool et al.'s (1987) model. This method was applied by Fu et al. (2005) in Yanhe watershed, China. Onori et al. (2006) used this model in Comunelli catchment, south-central Sicily, Italy. Yue-Qing et al. (2008) used it for Maotiao river watershed, Guizhou, south-western China.

Mcroberts et al. (2002) modified this model by introducing ratio of rill to the interrill erosion concept.

$$\mathrm{LS} = L \times S \times 1.4 \tag{55}$$

where $L = \left(\frac{\lambda}{\Psi}\right)^m$, $\lambda$ = flow path length (m or feet), $\lambda$ = (flow accumulation × cell size), $\Psi = 22.13$ for SI units and 72.6 for English units (BU) as the (LS) factor is the ratio of soil loss per unit area from a field slope to that from a 22.13 m length.

$$m = \beta/(1 + \beta) \tag{56}$$

$$\beta = (\sin\theta/0.0896)/[3.0 \times (\sin\theta)\,0.8 + 0.56] \quad (57)$$

$$S = 10\,\sin\theta + 0.03 \quad \text{if slope} < 9\% \quad (58)$$

$$S = 16.8\sin\theta - 0.05 \quad \text{if slope} \geq 9\% \quad (59)$$

where $\beta$ is the ratio of the rill erosion to the interrill erosion for conditions when the soil is moderately susceptible to both. $\theta$ is the angle of the slope in degree.

In India, Naqvi et al. (2012) adopted this model for Nun river watershed, Dehradun, Uttarakhand. Biswas and Pani (2015) used it for Barakar river basin, Jharkhand, India.

#### Desmet and Govers Slope Length Factor (*L*)

Most of the researchers have developed their slope steepness factor but borrowed the slope length factor from Wischmeier and Smith (1978a, b). Desmet and Govers (1996) developed a model for slope length factor ($L$).

$$L_{ij} = \frac{(A_{ij-in} + D^2)^{m+1} - A_{ij-in}^{m+1}}{D^{m+2} \cdot X_{ij}^{m} \cdot 22.13^{m}} \quad (60)$$

where $L_{ij}$ represents equivalent slope length factor for the cell, $A_{ij\,-\mathrm{in}}$ represents contributing area at the grid cell inlet, D represents the cell size, m represents the standard slope length exponent, $x_{ij}$ represents the contour length ($\sin\alpha_{ij}$ + $\cos\alpha_{ij}$) and $\alpha_{ij}$ is the direction of cell.

Lee and Lee (2006) applied this model Bosung basin, Korea. Mhangara et al. (2012) adopted modelling approach for Keiskamma catchment. Oliveira et al. (2015) used this method in his study in Ribeirão do Salto, a sub-basin of the Jequitinhonha Basin, located in Bahia State, Brazil.

## Variation of Cover Management Factor (*C*)

The vegetation cover is highly influential factor for soil erosion along with slope length and steepness factor Benkobi et al. (1994). The vegetation cover prevents the raindrops to impact on soil surface and dissipates the raindrop energy before reaching the soil surface. The value of $C$ depends upon the type of vegetation, growth stage of that vegetation and vegetation cover percentage.

USDA-SCS (1972) first developed the cover management factor depending upon water bodies, agricultural land, sparse vegetation, dense vegetation, barren land and built-up land (Table 1).

Later on, Rao (1981) adopted USDA-SCS (1972) concept for the determination of cover management factor for Indian context. Tirkey et al. (2013) used this concept for Daltonganj watershed, Palamu district, Jharkhand. Chatterjee et al. (2014) adopted this table for Upper Subarnarekha river basin, Jharkhand. Kamuju (2015) adopted this model for Gumani watershed, Jharkhand, India. Dahe and Borate (2015) used this model in Kaas Plateau of Maharashtra. Joshi et al. (2016) used the model for his study in the north of Pune, Maharashtra.

Wischmeier and Smith (1978a, b) modified USDA-SCS (1972) equation and generated more variation in land cover for C factor (Table 2).

Terranova et al. (2009) applied Wischmeier and Smith (1978a, b) table in Calabria, southern Italy, Europe. Bonilla et al. (2010) used this table in Santo Domingo County, Central Chile, South America. Efthimiou et al. (2014) used this for Venetikos river catchment, Western Macedonia, Northern Greece, Europe. Rozos et al. (2013) applied this model for North Euboea, Island, Greece, Europe. Kalambukattu and Kumar (2017) used model in Maniyar watershed, Uttarakhand, India. Gashaw et al. (2017a, b) used this model for Geleda watershed, Ethiopia.

Secretaria de Agricultura y Recursos Hidraulicos (1991) developed C factor from calculating the SLR (soil loss ratio) values (Table 3).

Then the C value for wet and dry season is calculated from this SLR. Millward and Mersey (1999) applied Secretaria de Agricultura y Recursos Hidraulicos (1991) model in Zenzontla sub-catchment, Rıo Ayuquıla watershed, Sierra de Manantlan Biosphere Reserve, south-western Mexico, USA.

Cai (1998) and Yang and Shi (1994) developed and established relationships between soil loss ratios and canopy cover and surface cover sub-factors. The cover management factor ($C$) of the RUSLE developed as a function of canopy/surface cover (c) in percentage is as follows:

$$C = 0.6508 - 0.343\,\log c \quad (61)$$

where $0 < c < 78.3\%$.

This model is used by Shi et al. (2004) for his study in Wangjiaqiao watershed, China.

Computation of $C$ factor was mostly approximation of $C$ factor on the basis of land cover types. In Morgan 1995, generated one model which shows the linear relationship between $C$ factor and NDVI (normalised difference vegetation index). McFarlane et al. (1991) developed the concept of NDVI:

$$C \text{ factor} = 1.02 - 1.21 \times \mathrm{NDVI} \quad (62)$$

where NDVI = (NIR − RED)/(NIR + RED).

Irvem et al. (2007) in his study on Seyhan river basin in Turkey used this concept. Agele et al. (2013) used this model for his study over Pahang river basin, Malaysia. Das and Guchait (2016) used it in Kharkai river basin, Jharkhand, India. Samanta et al. (2016) applied it for Subarnarekha river basin, Jharkhand, India. Pal and Shit (2017) used it for Jaipanda watershed, Bankura, West Bengal, India.

**Table 1** C factor developed by (USDA-SCS 1972)

| Land use and land cover class | *C* value |
|---|---|
| Built-up | 0.000 |
| Agricultural land | 0.400 |
| Dense vegetation | 0.004 |
| Sparse vegetation | 0.030 |
| Barren land | 1.000 |
| Water body | 0.000 |

**Table 2** C factor developed by (Wischmeier & Smith 1978)

| Land cover | *C* factor |
|---|---|
| Inland marshes | 0 |
| Salt marshes | 0 |
| Sclerophyllous vegetation | 0.005 |
| Broad-leaved forest | 0.001 |
| Coniferous forest | 0.001 |
| Mixed forest | 0.001 |
| Cultivation, with significant areas of natural vegetation | 0.05 |
| Non-irrigated arable land | 0.05 |
| Moors and heathland | 0.05 |
| Moors and heathland | 0.05 |
| Transitional woodland shrub | 0.05 |
| Sparsely vegetated areas | 0.05 |
| Discontinuous urban fabric | 0.05 |
| Industrial or commercial units | 0.05 |
| Mineral extraction sites | 0.05 |
| Fruit trees | 0.08 |
| Olive groves | 0.08 |
| Complex cultivation patterns | 0.08 |
| Natural grasslands | 0.1 |
| Burnt areas | 1 |
| Beaches, dunes, sands | 1 |

Renard et al. (1997) developed *C* factor relating to height of rain drop impact on ground surface after striking the canopy cover. And he termed it as canopy cover sub-factor.

$$CC = 1 - F_c(e^{-0.03048H}) \tag{63}$$

where CC is the canopy cover sub-factor ranging from 0 to 1, $F_c$ is fraction of canopy covered land surface and H (m) is distance of the raindrops fall after striking the canopy. Lopez-Vicente et al. (2008) adopted this equation for Central Spanish Pyrenees. In India, Naqvi et al. (2012) adopted this model for Nun river watershed, Dehradun, Uttarakhand.

Gutman and Ignatov (1998) developed another relationship between NDVI and the *C* factor.

$$C = 1 - \frac{\mathrm{NDVI} - \mathrm{NDVI}_{\min}}{\mathrm{NDVI}_{\max} + \mathrm{NDVI}_{\min}} \tag{64}$$

where NDVI is the NDVI of that pixel, $\mathrm{NDVI}_{\max}$ is the maximum NDVI value in that whole region in study and $\mathrm{NDVI}_{\min}$ is the minimum NDVI value in that whole region in study. Xu et al. (2013) applied this model for estimating *C* factor for the region surrounding the Bohai, Beijing City, Tianjin City, Hebei Province, Liaoning Province and Shandong Province.

Van et al. (2000) first observed that the *C* factor not linearly varies with NDVI. Actually, the *C* factor reduces exponentially with NDVI. He generated an exponentially decaying relationship between NDVI and *C* factor:

$$C = e^{(-\alpha(\mathrm{NDVI}/\beta - \mathrm{NDVI}))} \tag{65}$$

where $\alpha$, $\beta$ are parameters determining the shape of the NDVI-C curve.

A $\alpha$-value of 2 and a $\beta$-value of 1 seem to give reasonable results (Van et al. 2000) (Fig. 1).

Many Indian researchers used this formula for their work. Prasannakumar et al. (2011) used this equation for Siruvani river watershed, Attapady valley, Kerala. This model was adopted by Parveen and Kumar (2012) for Upper South Koel Basin, Jharkhand. Kartic et al. (2014) used this model in Kothagiri Taluk, Nilgiri, north-west part of the Tamil Nadu. Rahaman et al. (2015) applied this model in Kallar watershed, eastern part of Western Ghats, north-west part of the Tamil Nadu. Agarwal et al. (2016) used it for Khajuri watershed, Barkachha, Mirzapur, Uttar Pradesh. Baby and Nair (2016) used it for Kuttiyadi river basin, Northern Kerala. Markose and Jayappa (2016a, b) applied this equation for Kali river basin, Karnataka. Bhat et al. (2017) used for Kashmir valley.

**Table 3** C factor developed by (Secretaria de Agricultura y Recursos Hidraulicos 1991)

| Time period | Crop phase | SLR |
|---|---|---|
| November 10–March 10 | Harvest to ploughing or new seeding | 0.74 |
| March 10–April 1 | Seedbed preparation to 10% canopy cover | 0.77 |
| April 1–May 10 | Growth from 10% cover to 50% | 0.68 |
| May 10–June 20 | Growth from 50% cover to 75% | 0.49 |
| June 20–November 10 | Growth from 75% cover to harvest | 0.35 |

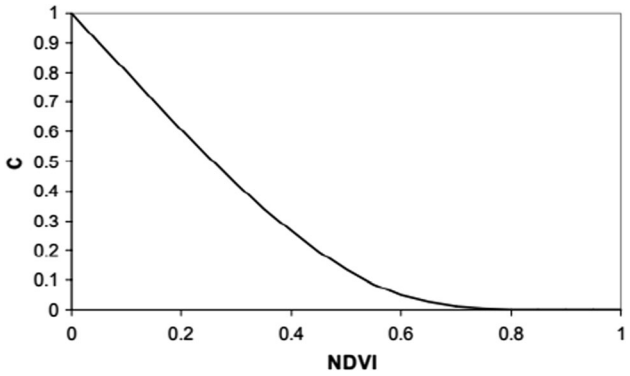


**Fig. 1** The exponential line used for C calculation from NDVI (Van et al. 2000)

Chen et al. (2008) introduced the back-propagation (BP) neural network for generating the cover management factor. According to Chen et al. (2008), the *C* factor is not only dependent upon NDVI, but it also depends upon the SAVI (soil-adjusted vegetation index) and he developed a neural network among all the indices to generate *C* factor (Fig. 2).

Chen et al. (2011) used this model in Miyun reservoir watershed, northern Beijing, North China. Samanta et al. (2016) applied it for Subarnarekha river basin, Jharkhand, India.

## Variation of Conservation Practice Factor (*P*)

The conservation or support practice factor (*P*) shows the effects of implementations that will reduce the rate and amount of the run-off, and thus, it reduces the amount and rate of soil erosion. The *P* factor reflects the proportion of soil loss for a particular support practice present for the corresponding soil loss with the presence of upward and downward slope, contour farming, tillage practice (Wischmeier and Smith 1957) (Renard et al. 1997). The

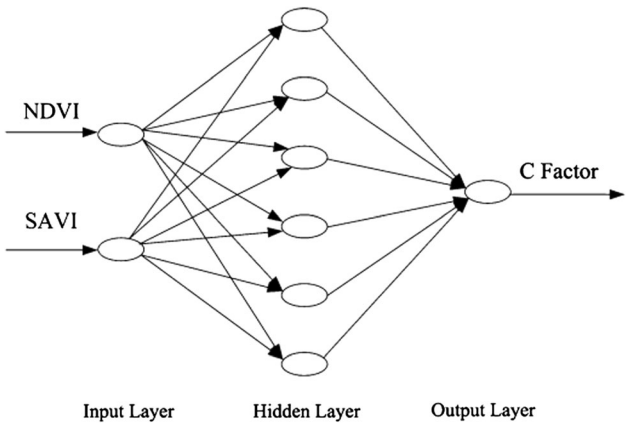


**Fig. 2** Back-propagation (BP) neural network by Chen et al. (2008)

common support practices are: contour farming, terracing, strip cropping, cross-slope cultivation and grassed waterways. As per Gitas (2009), the *P* values are calculated as the ratio of the rate and amount of soil loss due to a specific support practice to the soil loss due to row farming in upward and downward of the slope condition. The values of *P* factor range from 0 to 1. Among these values, the highest value is assigned to the areas where there is absence of any conservation practices (i.e. grasslands and open areas), and the minimum values given to plantation area with contour cropping and built-up land.

Development for the conservation practice factor (*P*) has not been elaborated till date; majorly the researchers used Wischmeier and Smith (1978a, b) concept for *P* factor in their study area. In Wischmeier and Smith 1978a, b, developed a *P* factor table which gives all types of conservation practice in consideration. Researchers can use that table for their particular study area without any difficulty.

At first, they have given the *P* factors for the area of contouring type of cultivation practice where ploughing and planting across a slope follow its contour lines. Water break created by these contour lines reduces the development of rills and gullies during the heavy water run-off. This is a major cause of soil erosion. For this type of area, Wischmeier and Smith (1978a, b) have given a table (Table 4).

Secondly, they have given *P* factors for strip cropping where the field is cultivated by partitioning the field into long, narrow strips. These striped fields are alternated in a crop rotation system. This method is used when there exists steeper slope or when there is absence of any alternative method for preventing soil erosion (Table 5).

In category "A" the *P* value is assigned to row crop for 4-year rotation, small grain with meadow seeding and 2 years of meadow. Another kind of row crop can be replaced by the small grain if meadow is established in it. In category "B" the *P* value is assigned for 4-year rotation of 2-year row crop, winter grain with meadow seeding and

**Table 4** *P* factor for contour ploughing developed by (Wischmeier and Smith 1978a, b)

| Land slope percentage (%) | *P* value | Maximum length (Feet) |
|---|---|---|
| 1–2 | 0.6 | 400 |
| 3–5 | 0.5 | 300 |
| 6–8 | 0.5 | 200 |
| 9–12 | 0.6 | 120 |
| 13–16 | 0.7 | 80 |
| 17 – 20 | 0.8 | 60 |
| 21 – 25 | 0.9 | 50 |

**Table 5** *P* factor for strip cropping developed by (Wischmeier and Smith 1978a, b)

| Land slope percentage (%) | *P* value | | | Strip width (Feet) | Maximum length (Feet) |
|---|---|---|---|---|---|
| | A | B | C | | |
| 1–2 | 0.30 | 0.45 | 0.60 | 130 | 800 |
| 3–5 | 0.25 | 0.38 | 0.50 | 100 | 600 |
| 6–8 | 0.25 | 0.38 | 0.50 | 100 | 400 |
| 9–12 | 0.30 | 0.45 | 0.60 | 80 | 240 |
| 13–16 | 0.35 | 0.52 | 0.70 | 80 | 160 |
| 17–20 | 0.40 | 0.60 | 0.80 | 60 | 120 |
| 21–25 | 0.45 | 0.68 | 0.90 | 50 | 100 |

1-year meadow. "C" category is for alternate strips of row crop and small grain crop.

Next, Wischmeier and Smith (1978a, b) developed *P* factor for terracing type of cultivation practice where agricultural field has been cut into a series of successively receding flat surfaces or platforms as a form of steps, for the purposes of more effective farming. This type of farming is commonly used to farm on hilly or mountainous region. Terraced fields decrease both surface run-off and erosion (Table 6).

Bewket and Teferi (2009) used Wischmeier and Smith (1978a, b) model in his study on Chemoga watershed, Blue Nile basin in the Northwest Highlands of Ethiopia. In India Dahe and Borate (2015) applied this model in Kaas Plateau of Maharashtra. Joshi et al. (2016) used the model for his study in the north of Pune, Maharashtra. Gelagay (2016) used this model for Koga watershed, Upper Blue Nile Basin, Ethiopia, North East Africa; Gashaw et al. (2017a, b) used this model for Geleda watershed, Ethiopia.

Wener (1981) developed an equation that produces the linear interconnection between slope (S) of the area and the amount of conservation practice (*P*):

$$P = 0.2 + 0.03 \times S \tag{66}$$

where *P* is amount of conservation practice; S is the percentage of slope.

Lufafa et al. (2003) used this equation in his study on Lake Victoria basin, Kenya, eastern Africa. Fu et al. (2005) used this model in Yanhe watershed, China. Terranova et al. (2009) applied Sorrentino's (2001) model in Calabria, Italy, Europe.

In India, Parveen and Kumar (2012) modified Wischmeier and Smith (1978a, b) model of conservation practice for Upper South Koel Basin, Jharkhand (Table 7).

Agarwal et al. (2016) used it for Khajuri watershed, Barkachha, Mirzapur, Uttar Pradesh.

But majorly in all over the world, the conservation practice is taken as unity due to the absence of proper conservation practice.

## Analysis of RUSLE Model Through the Application of GIS and Remote Sensing

After choosing the proper model for each and individual RUSLE parameters from the previous review as per the study area requirement, each and individual parameters are analysed by GIS and remote sensing technology as this technology solves the problem in less time and low cost of estimation rather than other field-based general computational techniques.

### Analysis of Rainfall Erosivity Factor (*R*) with the Help of GIS

In any GIS environment, the rainfall data can be interpolated through kriging interpolation method as kriging

**Table 6** *P* factor for terracing developed by (Wischmeier and Smith 1978a, b)

| Land slope percentage (%) | Farm planning | | Computing sediment yield | |
|---|---|---|---|---|
| | Contour factor | Strip crop factor | Graded channels sod outlets | Steep back slope underground outlets |
| 1–2 | 0.60 | 0.30 | 0.12 | 0.05 |
| 3–8 | 0.50 | 0.25 | 0.10 | 0.05 |
| 9–12 | 0.60 | 0.30 | 0.12 | 0.05 |
| 13–16 | 0.70 | 0.35 | 0.14 | 0.05 |
| 17–20 | 0.80 | 0.40 | 0.16 | 0.06 |
| 21–25 | 0.90 | 0.45 | 0.18 | 0.06 |

**Table 7** *P* factor for contour cropping, strip cropping and terracing developed by Parveen and Kumar (2012)

| Slope | Contouring | Strip cropping | Terracing |
|---|---|---|---|
| 0.0–7.0 | 0.55 | 0.27 | 0.10 |
| 7.0–11.3 | 0.60 | 0.30 | 0.12 |
| 11.3–17.6 | 0.80 | 0.40 | 0.16 |
| 17.6–26.8 | 0.90 | 0.45 | 0.18 |
| >26.8 | 1.00 | 0.50 | 0.20 |

method produced the lowest error across all in one time period, showed consistent performance and provided reliable estimates regardless of the number of gages or the cell size used in the interpolation (Mair and Fares 2011). Now this interpolated rainfall data are used to generate the proper rainfall erosivity factor (*R*) as per the climatic condition of the study area.

## Analysis of Soil Erodibility Factor (*K*) with the Help of GIS

The soil type data can be collected from the regional soil survey and land research department. These data can be imported to GIS environment where extraction of the soil groups can be done. After extraction of groups, the soil properties (i.e. organic content, particle size distribution, permeability, structural parameters of soil) can be tested and determined through the field sampling of soils from the study area. Now this estimated soil properties for each and individual soil groups can be further processed for the calculation of *K* factor as per the chosen *K* factor model.

## Analysis of Slope Length and Steepness Factor (LS) with the Help of GIS

The slope of the study area can be calculated by two methods. The toposheet collected from the regional topological survey department gives the contours. These contours are digitised in GIS. These digitised contours give the digital elevation model (DEM) by using raster interpolation technique in GIS. There are various interpolation techniques; among them IDW (inverse distance weighting) and NN (nearest neighbour) interpolation methods are best suitable for geo-morphologically smooth areas (Arun 2013). This DEM is used to generate slope of that area. When the contours from toposheet do not give the proper slope pattern, then the SRTM (Shuttle Radar Topography Mission) DEM and CARTOSAT DEM can be used to generate slope. The flow direction raster is generated from the DEM. From this flow direction raster, the flow accumulation raster of that study area is generated. This flow accumulation raster and slope are used to generate the slope length and steepness factor (LS) (as per the model chosen) using raster calculator tool of ArcGIS.

## Analysis of Cover Management Factor (*C*) with the Help of GIS and Remote Sensing

The land use and land cover are classified from the satellite imagery data with the help of supervised classification technique of remote sensing technology. From this classification, the *C* factor is assigned in GIS. Otherwise, the NDVI (normalised difference vegetation index) generated from the satellite imagery is used to generate *C* factor distribution as per the chosen model.

## Analysis of Conservation Practice Factor (*P*) with the Help of GIS and Remote Sensing

At first, the study area must be visited to observe that there is presence of any conservation practice (i.e. contour cropping, strip cropping, terracing, tillage practice) or not. If there exists any kind of conservation practice, then the proper *P* factor value is assigned for that particular area with respect to their slope. If no conservation practice is present, the *P* factor is taken as 1.

After the estimation of all factors for the study area, the factors can be overlaid in GIS which gives the spatial variation of soil loss per year over that area.

## References

Adediji, A., Tukur, A., & Adepoju, K. (2010). Assessment of revised universal soil loss equation (RUSLE) in Katsina Area, Katsina State of Nigeria using remote sensing (RS) and geographic information system (GIS). *Iranica Journal of Energy & Environment, 1*(3), 255–264.

Agarwal, D., et al. (2016). Soil erosion mapping of watershed in Mirzapur district using RUSLE model in GIS environment. *International Journal of Students' Research In Technology & Management, 4*(3), 56–63.

Agele, D., Lihan, T., Sahibin, A., & Rahman, Z. (2013). Application of the RUSLE model in forecasting soil erosion at downstream of the Pahang river basin, Malaysia. *Journal of Applied Sciences Research, 9*(1), 413–424.

Amsalu, T., & Mengaw, A. (2014). GIS based soil loss estimation using RUSLE model: The case of Jabi Tehinan Woreda, ANRS, Ethiopia. *Natural Resources, 5,* 616–626.

Angima, S., et al. (2003). Soil erosion prediction using RUSLE for central Kenyan highland conditions. *Agriculture, Ecosystems & Environment, 97,* 295–308.

Arnoldus, H., Boodt, M. & Gabriels, D., (1980). *An approximation of the rainfall factor in the Universal Soil Loss Equation.* s.l.:s.n.

Babu, R., Dhyani, B., & Kumar, N. (2004). Assessment of erodibility status and refined Iso- erodent map of India. *Indian Journal of Soil Conservation, 32*(2), 171–177.

Babu, R., Tejwani, K., Agrawal, M. & Bhusan, L., (1979). Rainfall intensity duration-return equation and nomographs of India.

Baby, A., & Nair, A. (2016). Soil erosion estimation of Kuttiyadi River Basin Using RUSLE. *International Advanced Research Journal in Science, Engineering and Technology, 3*(3), 275–279.

Benkobi, L., Trlica, M., & Smith, J. (1994). Evaluation of a redefined surface cover sub-factor for use in RUSLE. *Journal of Range Management, 47,* 74–78.

Bewket, W., & Teferi, E. (2009). Assessment of soil erosion hazard and prioritization for treatment at the watershed level: Case study in the Chemoga watershed, Blue Nile Basin, Ethiopia. *Land Degradation & Development, 20,* 609–622.

Bhandari, K., & Darnsawasdi, R. (2015). Application of remote sensing and participatory soil erosion assessment approach for soil erosion mapping in a watershed. *Walailak Journal of Science and Technology, 12*(8), 689–702.

Bhat, S., et al. (2017). Soil erosion modeling using RUSLE & GIS on micro watershed of J&K. *Journal of Pharmacognosy and Phytochemistry, 6*(5), 838–842.

Biswas, S. S., & Pani, P. (2015). Estimation of soil erosion using RUSLE and GIS techniques: A case study of Barakar River basin, Jharkhand. *India. Modeling Earth Systems and Environment, 1*(4), 1–13.

Bonilla, C. A., Reyes, J. L., & Magri, A. (2010). Water erosion prediction using the revised universal soil loss equation (RUSLE) in a GIS framework, Central Chile. *Chilean Journal of Agricultural Research, 70*(1), 159–169.

Bu, Z., et al. (2003). The progress of quantitative remote sensing method for annual soil losses and its application in Taihu-Lake Watersheds. *Acta Pedol Sin, 40*(1), 1–9. **(in Chinese)**.

Cai, C. (1998). *Prediction of nutrients loss caused by soil erosion and assessment of fertility with GIS at small watershed level*. PhD thesis.

Chatterjee, S., Krishna, A. P., & Sharma, A. P. (2014). Geospatial assessment of soil erosion vulnerability at watershed level in some sections of the Upper Subarnarekha river basin, Jharkhand, India. *Environmental Earth Sciences, 71,* 357–374.

Chen, T., Li, P. & Zhang, L., (2008). *Retrieving vegetation cover by using BP neural network based on ''Beijing-1'' microsatellite data. China*. In The International conference on earth observation data processing and analysis (ICEODPA2008).

Chen, T., et al. (2011). Regional soil erosion risk mapping using RUSLE, GIS, and remote sensing a case study in Miyun Watershed, North China. *Environmental Earth Sciences, 63,* 533–541.

Dahe, P., & Borate, P. (2015). Development of erosion hotspots for Kaas Plateau (ESZ) of Western Ghat, Maharashtra using RUSLE and arc GIS. *International Journal of Remote Sensing & Geoscience (IJRSG), 4*(4), 35–43.

Das, G., & Guchait, R. (2016). Modeling of risk of soil erosion in Kharkai Watershed using RUSLE and TRMM Data: A geospatial approach. *International Journal of Science and Research (IJSR), 5*(10), 1–10.

Demirci, A., & Karaburun, A. (2012). Estimation of soil erosion using RUSLE in a GIS framework a case study in the Buyukcekmece Lake watershed, northwest Turkey. *Environmental Earth Sciences, 66,* 903–913.

Desmet, P., & Govers, G. (1996). A GIS-procedure for the automated calculation of the USLE LS-factor on topographically complex landscape units. *Journal of Soil and Water Conservation, 51*(5), 427–433.

Diodato, N. (2004). Estimating Rusle's rainfall factor in the part of Italy with a Mediterranean rainfall regime. *Hydrology and Earth System Sciences, 8,* 103–107.

Efthimiou, N., Lykoudi, E., & Karavitis, C. (2014). Soil erosion assessment using the RUSLE model and GIS. *European Water, 47,* 15–30.

El-Swaify, S., & Dangler, E. (1976). Erodibilities of selected tropical soils in relation to structural and hydrologic parameters. In G. Foster (Ed.), *Soil Erosion Prediction and Control* (pp. 105–114). Ankeny: Soil and Water Conservation Society.

Ferro, V., Giordano, G., & Lovino, M. (1991). Isoerosivity and erosion risk map for Sicily. *Hydrological Sciences Journal, 36*(6), 549–564.

Flabouris, K. (2008). *Study of rainfall factor R on the RUSLE law*.

Foster, G., McCool, D., Renard, K., & Moldenhauer, W. (1981). Conversion of the universal soil loss equation to SI metric units. *Journal of Soil and Water Conservation, 36*(6), 355–359.

Foster, G., Meyer, L., & Onstad, C. (1977). An erosion equation derived from basic erosion principles. *Transactions of the ASAE, 20*(4), 683–687.

Fu, B. J., et al. (2005). Assessment of soil erosion at large watershed scale Using RUSLE and GIS: A case study in the Loess Plateau of China. *Land Degradation & Development, 16,* 73–85.

Ganasri, B., & Ramesh, H. (2016). Assessment of soil erosion by RUSLE model using remote sensing and GIS—A case study of Nethravathi Basin. *Geoscience Frontiers, 7,* 953–961.

Gashaw, T., Tulu, T., & Argaw, M. (2017). Erosion risk assessment for prioritization of conservation measures in Geleda watershed, Blue Nile basin, Ethiopia. *Environmental Systems Research, 6*(1), 1–14.

Gashaw, T., Tulu, T., & Argaw, M. (2017b). Erosion risk assessment for prioritization of conservation measures in Geleda watershed, Blue Nile basin, Ethiopia. *Environmental Systems Research, 6*(1), 1–14.

Gaudasasmita, K. (1987). *Contribution to geo-information system operation for prediction of erosion.* ITC, Netherlands: s.n.

Gelagay, H. (2016). RUSLE and SDR model based sediment yield assessment in a GIS and remote sensing environment: A case study of Koga Watershed, Upper Blue Nile Basin, Ethiopia. *Hydrology Current Research, 7*(2), 239.

Ghosh, K. G., Mukhopadhyay, S., & Pal, S. (2015). Surface runoff and soil erosion dynamics: A case study on Bakreshwar river basin, eastern India. *International Research Journal of Earth Sciences, 3*(7), 11–22.

Gitas, I. et al. (2009). *Multi-temporal soil erosion risk assessment in N. Chalkidiki using a modified USLE raster model.* s.l., In EARSeL eProceedings (pp. 40–52).

Goldman, S., & Wischmeier, W. (1986). *Erosion and sediment control handbook*. New York: McGraw Hill.

Gutman, G., & Ignatov, A. (1998). The derivation of the green vegetation fraction from NOAA/AVHRR data for use in numerical weather prediction models. *International Journal of Remote Sensing, 19*(8), 1533–1543.

Hammad, A. A., Lundekvam, H., & Børresen, T. (2005). Adaptation of RUSLE in the eastern part of the mediterranean region. *Environmental Management, 34*(6), 829–841.

Helden, U. (1987). *An assessment of woody biomass, community forests, land use and soil erosion in Ethiopia*. s.l.: Lund University Press.

Hickey, R. (2000). Slope angle and slope length solutions for GIS. *Cartography, 29,* 1–8.

Hurni, H. (1985). *Soil conservation manual for Ethiopia*.

ICONA, (1988). *Agresividad de la lluvia en España.* Madrid, España, Servicio de Publicaciones del Ministerio de Agricultura, Pesca y Alimentación (p. 39).

Irvem, A., Topalog˘lu, F., & Uygur, V. (2007). Estimating spatial distribution of soil loss over Seyhan River Basin in Turkey. *Journal of Hydrology, 336,* 30–37.

Joshi, V., Susware, N., & Sinha, D. (2016). Estimating soil loss from a watershed in Western Deccan, India, using Revised Universal Soil Loss Equation. *Landscape & Environment, 10*(1), 13–25.

Kalambukattu, J., & Kumar, S. (2017). Modelling soil erosion risk in a mountainous watershed of Mid-Himalaya by integrating RUSLE model with GIS. *Eurasian Journal of Soil Science, 6*(2), 92–105.

Kamuju, N. (2015). A study on estimation and comparison of average annual soil erosion with different slope length [L] and Steepness factors[S] by RUSLE model using remote sensing and GIS technology. *IJITR International Journal of Innovative Technology and Research, 3*(5), 2424–2431.

Kamuju, N. (2016). spatial identification and classification of soil erosion prone zones using remote sensing & gis integrated 'rusle' model and 'sateec gis system. *International journal of engineering sciences & research technology, 5*(10), 676–686.

Kartic, K. M., Annadurai, R., & Ravichandran, T. (2014). Assessment of soil erosion susceptibility in Kothagiri. *International Journal of Scientific and Research Publications Taluk Using Revised Universal Soil Loss Equation (RUSLE) and Geo-Spatial Technology*, *4*(10), 1–13.

KICT, (1992). The development of selection standard for calculation method of unit sediment yield in rivers. *KICT 89-WR-113.*

Kim, S.-M., et al. (2012). Estimation of soil erosion and sediment yield from mine tailing dumps using GIS: a case study at the Samgwang mine, Korea. *Geosystem Engineering, 15*(1), 2–9.

Kumar, S., & Kushwaha, S. (2013). Modelling soil erosion risk based on RUSLE-3D using GIS in a Shivalik sub-watershed. *Journal of Earth System Science, 122*(2), 389–398.

Lee, G., & Lee, K. (2006). Scaling effect for estimating soil loss in the RUSLE model using remotely sensed geospatial data in Korea. *Hydrology and Earth System Sciences, 3,* 135–157.

Lema, B., et al. (2016). Use of the revised universal soil loss equation (RUSLE) for soil and nutrient loss estimation in long-used rainfed agricultural lands, North Ethiopia. *Physical Geography, 37*(3–4), 276–290.

Lopez-Vicente, M., Navas, A., & Machín, J. (2008). Identifying erosive periods by using RUSLE factors in mountain fields of the Central Spanish Pyrenees. *Hydrology and Earth System Sciences, 12,* 523–535.

Loureiro, N., & Coutinho, M. (2001). A new procedure to estimate the RUSLE EI30 index, based on monthly rainfall data and applied to the Algarve region, Portugal. *Journal of Hydrology, 250,* 12–18.

Lufafa, A., et al. (2003). Prediction of soil erosion in a Lake Victoria basin catchment using a GIS-based Universal Soil Loss model. *Agricultural Systems, 76,* 883–894.

Maria, K., Pantelis, S., & Filippos, V. (2009). Soil erosion prediction using the Revised Universal soil loss equation (RUSLE) in a GIS framework, Chania, Northwestern Crete, Greece. *Environmental Geology, 57,* 483–497.

Markose, V. & Jayappa, K., (2016). Soil loss estimation and prioritization of sub-watersheds of Kali River basin, Karnataka, India, using RUSLE and GIS. *Environmental Monitoring and Assessment*. https://doi.org/10.1007/s10661-016-5218-2.

Markose, V., & Jayappa, K. (2016b). Soil loss estimation and prioritization of sub-watersheds of Kali River basin, Karnataka, India, using RUSLE and GIS. *Environmental Monitoring and Assessment, 188*(4), 1–16.

McCool, D., Brown, L., Foster, G., & Mutchler, L. (1987). Revised slope steepness factor for the Universal Soil Loss Equation. *Transactions of the ASAE (American Society of Agricultural Engineers), 30,* 1387–1396.

McFarlane, D., Delroy, N., & Van, S. V. (1991). Water erosion of potato land in Western Australia. *Australian journal of soil and water conservation*, *4*(1), 33–40.

Mcroberts, R., Nelson, M., & Wendt, D. (2002). Stratified estimation of forest area using satellite imagery, inventory data, and the kNearest Neighbors technique. *Remote Sensing of Environment, 82,* 457–468.

Mhangara, P., Kakembo, V., & Lim, K. (2012). Soil erosion risk assessment of the Keiskamma catchment, South Africa using GIS and remote sensing. *Environmental Earth Sciences, 65*(7), 2087–2102.

Millward, A. A., & Mersey, J. E. (1999). Adapting the RUSLE to model soil erosion potential in a mountainous tropical watershed. *Catena, 38,* 109–129.

Moore, I., & Burch, F. (1986). Physical basic of the length–slope factor in the Universal Soil Loss Equation. *Soil Science Society of America Journal, 50,* 1294–1298.

Morgan, R. P. C. (1986). *Soil erosion and conservation*. s.l.: Longman.

Morgan, R. (1995). *Soil Erosion and Conservation* (2nd ed.). UK: Longman.

Morgan, R., & Davidson, D. (1991). *Soil Erosion and Conservation*. UK: Longman Group.

Mulengera, M., & Payton, R. (1999). Estimating the USLE-soil erodibility factor in developing tropical countries. *Trop Agric (Trinidad), 76*(1), 17–22.

Naqvi, H. R., Devi, L. M., & Siddiqui, M. A. (2012). Soil loss prediction and prioritization based on revised universal soil loss estimation (RUSLE) model using geospatial technique. *International Journal of Environmental Protection, 2*(3), 39–43.

Oliveira, J. A., Dominguez, J. M. L., Nearing, M. A., & Oliveira, P. T. S. (2015). A GIS-based procedure for automatically calculating soil loss from the universal soil loss equation: Gisus-m. *American Society of Agricultural and Biological Engineers, 31*(6), 907–917.

Onori, F., Bonis, P. D., & Grauso, S. (2006). Soil erosion prediction at the basin scale using the revised universal soil loss equation (RUSLE) in a catchment of Sicily (southern Italy). *Environmental Geology, 50,* 1129–1140.

Pal, S., & Shit, M. (2017). Application of RUSLE model for soil loss estimation of Jaipanda watershed, West Bengal. *Spatial Information Research, 25*(3), 399–409.

Parveen, R., & Kumar, U. (2012). Integrated approach of universal soil loss equation (USLE) and geographical information system (GIS) for soil loss risk assessment in Upper South Koel Basin, Jharkhand. *Journal of Geographic Information System, 4,* 588–596.

Parysow, P., Wang, G., Gertner, G., & Anderson, A. (2003). Spatial uncertainty analysis for mapping soil erodibility based on joint sequential simulation. *CATENA, 53,* 65–78.

Prasannakumar, V., Shiny, R., Geetha, N., & Vijith, H. (2011). Spatial prediction of soil erosion risk by remote sensing, GIS and RUSLE approach: a case study of Siruvani river watershed in Attapady valley, Kerala, India. *Environmental Earth Sciences, 64,* 965–972.

Rahaman, S., Aruchamy, S., Jegankumar, R., & Ajeez, S. (2015). Estimation of annual average soil loss, based on RUSLE model in Kallar watershed, Bhavani basin, Tamil Nadu, India. *ISPRS Annals of the Photogrammetry, Remote Sensing and Spatial Information Sciences*, *II-2/W2*, 207–214.

Ramu, M., & Mahalingam, B. (2015). Quantification of soil erosion by water using GIS and remote sensing techniques: A study of Pandavapura Taluk, Mandya district, Karnataka, India. *ARPN Journal of Earth Sciences, 4*(2), 103–110.

Ranzi, R., Le, T. H., & Rulli, M. C. (2012). A RUSLE approach to model suspended sediment load in the Lo river (Vietnam): Effects of reservoirs and land use changes. *Journal of Hydrology, 422–423,* 17–29.

Rao, Y., (1981). *Evaluation of cropping management factor in universal soil loss equation under natural rainfall condition of Kharagpur, India.* Bangkok, Proceedings of the Southeast Asian Regional Symposium on Problems of Soil Erosion and Sedimentation, Asian Institute of Technology (AIT), (p. 241–254).

Renard, K., Foster, G., Weesies, G. & McCool, (1997). Predicting soil erosion by water: a guide to conservation planning with the Revised Universal Soil Loss Equation RUSLE. *Handbook No. 703. US Department of Agriculture,* (pp. 404).

Renard, K., & Freimund, J. (1994). Using monthly precipitation data to estimate the R-factor in the RUSLE. *Journal of Hydrology, 157,* 287–306.

Römkens, M., Prasad, S., & Poesen, J. (1986). *Soil erodibility and properties* (pp. 492–504). s.n.: Hamburg.

Roose, E., (1975). *Érosion et ruissellement en afrique de l'ouest vingt années de mesures en petites parcelles expérimentales.* cyclo: orstom.

Roose, E., (1996). *Land Husbandry-Components and strategy,* s.l.: FAO Corporate Document Repository 70 FAO Soil Bulletin ISBN 92-5-103451-6. Chapter 5.

Rosewell, C. (1993). *Soilloss—A program to assist in the selection of the management practices to reduce erosion* (2nd ed.). s.l.: Soil Conservation Service of New South Wales.

Rozos, D., Skilodimou, H. D., Loupasakis, C., & Bathrellos, G. D. (2013). Application of the revised universal soil loss equation model on landslide prevention. An example from N. Euboea (Evia) Island, Greece. *Environmental Earth Sciences, 70,* 3255–3266.

Samanta, R., Bhunia, G., & Shit, P. (2016). Spatial modelling of soil erosion susceptibility mapping in lower basin of Subarnarekha river (India) based on geospatial techniques. *Modeling Earth Systems and Environment*, *2*(99), 1–13.

Santra, P., Goyal, R., Tewari, J., & Roy, M. (2014). *Assessment of potential soil loss rate by wind and water erosion in Jodhpur region of western Rajasthan*. India: Global Soil Map.

Schwab, G. O., Fangmeier, D. D. & Elliot, W. J., (1994). *Soil and Water Conservation Engineering.* fourth ed. s.l.:s.n.

Schwab, G., Frevert, R., & Edminster, T. (1981). *Soil water conservation engineering* (3rd ed.). New York: Wiley.

Secretaria de Agricultura y Recursos Hidraulicos, (1991). *Manual de Prediccion de Peridas de Suelo por Erosion,* Colegio de Postgraduados, Guadalajara, 115 pp: s.n.

Sewnet, G. H. (2016). USLE and SDR Model Based Sediment Yield Assessment in a GIS and Remote Sensing Environment; A Case Study of Koga Watershed, Upper Blue Nile Basin. *Ethiopia. Hydrology Current Research, 7*(2), 1–10.

Sharpley, A., & Williams, J. (1990). *EPIC-erosion/productivity impact calculator: 1. model documentation* (p. 1768). Washington: US Department of Agriculture Technical Bulletin No.

Shi, Z. H., Cai, C. F., Ding, S. W., Wang, T. W., & Chow, T. L. (2004). Soil conservation planning at the small watershed level using RUSLE with GIS: a case study in the Three Gorge Area of China. *CATENA, 55,* 33–48. https://doi.org/10.1016/S0341-8162(03)00088-2.

Shinde, V., Tiwari, K., & Singh, M. (2010). Prioritization of micro watersheds on the basis of soil erosion hazard using remote sensing and geographic information system. *International Journal of Water Resources and Environmental Engineering, 2*(3), 130–136.

Shit, P., Nandi, A. & Bhunia, G. (2015). Soil erosion risk mapping using RUSLE model on jhargram sub-division at West Bengal in India. *Modeling Earth Systems and Environment*. https://doi.org/10.1007/s40808-015-0032-3.

Sigalos, G., Loukaidi, V., Dasaklis, S. & Alexouli-Livaditi, A., (2010). *Assessment of the quantity of the material transported downstream of Sperchios river, central Greece,* Patras: Bulletin of the Geological Society of Greece, 2010, Proceedings of the 12th International Congress.

Simms, A. D., Woodroffe, C. D. & Jones, B. G. (2003). *Application of RUSLE for erosion management in a coastal catchment, Southern NSW*. International Congress on Modelling and Simulation, July, Volume 2, (pp. 678–683).

Singh, G. (1981). *Soil loss and pre-diction research in India*. Dehra Dun: Central Soil and Water Conservation Research Training Institute.

Sorrentino, G. (2001). *Indagine regionale sulla stima dell'aggressività della pioggia nello studio dell'erosione idrica* (p. 222). Cosenza: Thesis, Università degli Studi della Calabria, Facoltà di Ingegneria.

Swarnkar, S., Malini, A., Tripathi, S., & Sinha, R. (2017). Assessment of uncertainties in soil erosion and sediment yield estiamtes at ungauged basins: an application to the Garra River basin. *India. Hydrology and Earth System Sciences*, *22*(4), 2471–2485.

Terranova, O., Antronico, L., Coscarelli, R., & Iaquinta, P. (2009). Soil erosion risk scenarios in the Mediterranean environment using RUSLE and GIS: An application model for Calabria (southern Italy). *Geomorphology, 112,* 228–245.

Tew, K. (1999). *Production of Malaysian soil erodibility nomograph in relation to soil erosion issues.* 27 ed. Jalan SS 14/2D, 47500 Subang Jaya, Selangor DarulEhsan, Malaysia: VT SoilErosion Research & Consultancy.

Tirkey, A. S., Pandey, A., & Nathawat, M. (2013). Use of satellite data, GIS and RUSLE for estimation of average annual soil loss in daltonganj watershed of Jharkhand (India). *Journal of Remote Sensing Technology, 1*(1), 20–30.

Torri, D., Poesen, J., & Borselli, L. (1997). Predictability and uncertainty of the soil erodibility factor using a global dataset. *CATENA, 31,* 1–22.

USDA, (1951). Soil survey manual. In *Soil Conservation Service, Soil Survey Staff, U.S. Dept. of Agricultural handbook 18.* (p. 503). Washington D.C., USA: U.S. Govt. Print Office.

USDA-SCS. (1972). *'Hydrology' in SCS national engineering handbook, section 4*. Washington DC: US Department of Agriculture.

Van, R. R., Hamilton, M., & Hickey, R. (2001). Estimating the LS Factor for RUSLE through iterative slope length processing of digital elevation data within ArcInfo Grid. *Cartography, 30*(1), 27–35.

Van, D. K. J., Jones, R., & Montanarella, L. (2000). *Soil erosion risk assessment in Europe*. Luxembourg: Office for Official Publications of the European Communities.

Vezina, K., Bonn, F., & Pham, V. (2006). Agricultural land-use patterns and soil erosion vulnerability of watershed units in Vietnam's northern highlands. *Landscape Ecology, 21*(8), 1311–1325.

Vinay, M., Ramu & Mahalingam, B., (2015). Quantification of soil erosion by water using GIS and remote sensing techniques: A study of Pandavapura Taluk, Mandya District, Karnataka. *India. ARPN Journal of Earth Sciences*, *4*(2), 103–110.

Wener, C. (1981). *Soil conservation in Kenya*. Nairobi: Ministry of Agriculture, Soil Conservation Extension Unit.

Wischmeier, W., & Smith, D. (1957). Factors affecting sheet and rill erosion. *Transactions. American Geophysical Union, 38*(6), 889–896.

Wischmeier, W. & Smith, D., 1978. Predicting rainfall erosion losses—A guide to conservation planning. *Agriculture Handbook No.537,* pp. 3–4.

Wischmeier, W. & Smith, D., (1978). *Predicting rainfall erosion losses—A guide to conservation planning.* s.l.:USDA Agricultural Handbook No. 537.

Xu, L., Xu, X., & Meng, X. (2013). Risk assessment of soil erosion in different rainfall scenarios by RUSLE model coupled with

information diffusion model: A case study of Bohai Rim, China. *CATENA, 100,* 74–82.

Xu, L., et al. (2007). Simple method of estimating rainfall erosivity under different rainfall amount of Beijing. *Research of Soil and Water Conservation, 6,* 398–402.

Yang, Y. & Shi, D., (1994). Study on Soil Erosion in the Three Gorge Area of the Changjiang River.

Yu, B., & Rosewell, C. J. (1998). Rainfall erosivity and its estimation for Australia's tropics. *Australian Journal of Soil Research, 36,* 143–165.

Yue-Qing, X., et al. (2008). Adapting the RUSLE and GIS to model soil erosion risk in a mountains karst watershed, Guizhou Province, China. *Environmental Monitoring and Assessment, 141,* 275–286.

Zarris, D., Vlastara, M., & Panagoulia, D. (2011). Sediment delivery assessment for a transboundary mediterranean catchment: The example of Nestos River Catchment. *Water Resources Management, 25,* 3785–3803.

Zhao, W., Fu, B., Chen, L. & Zhang, Q. (2004). Estimation of rainfall erosivity using rainfall amount: a case study in hilly and gully area of Loess Plateau in northern Shaanxi. *Land Change and Eco-environmental Construction.*